Cardiac-specific overexpression of RhoA results in sinus and atrioventricular nodal dysfunction and contractile failure

Valerie P. Sah,[1] Susumu Minamisawa,[2] Steven P. Tam,[1] Thomas H. Wu,[1] Gerald W. Dorn II,[3] John Ross Jr.,[2] Kenneth R. Chien,[2] and Joan Heller Brown[1]

[1]Department of Pharmacology, and
[2]Department of Medicine, University of California–San Diego, La Jolla, California 92093, USA
[3]Department of Medicine, University of Cincinnati, Cincinnati, Ohio 45267, USA

Address correspondence to: Joan Heller Brown, Department of Pharmacology, University of California–San Diego, 9500 Gilman Drive, La Jolla, California 92093-0636, USA. Phone: (858) 534-2595; Fax: (858) 822-0041; E-mail: jhbrown@ucsd.edu.

Received for publication March 17, 1999, and accepted in revised form May 18, 1999.

RhoA is a low-molecular-weight GTPase that has been implicated in the regulation of hypertrophic cardiac muscle cell growth. To study the role of RhoA in control of cardiac function in vivo, transgenic mice expressing wild-type and constitutively activated forms of RhoA under the control of the cardiac-specific α-myosin heavy chain promoter were generated. Transgene-positive mice expressing high levels of either wild-type or activated RhoA showed pronounced atrial enlargement and manifested a lethal phenotype, often preceded by generalized edema, with most animals dying over the course of a few weeks. Echocardiographic analysis of visibly healthy wild-type RhoA transgenic mice revealed no significant change in left ventricular function. As their condition deteriorated, significant dilation of the left ventricular chamber and associated decreases in left ventricular contractility were detected. Heart rate was grossly depressed in both wild-type and activated RhoA-expressing mice, even prior to the onset of ventricular failure. Electrocardiography showed evidence of atrial fibrillation and atrioventricular block. Interestingly, muscarinic receptor blockade with atropine did not elicit a positive chronotropic response in the transgenic mice. We suggest that RhoA regulates cardiac sinus and atrioventricular nodal function and that its overexpression results in bradycardia and development of ventricular failure.

J. Clin. Invest. **103**:1627–1634 (1999).

Introduction

When an increased workload is placed on the heart, compensatory mechanisms are activated to preserve myocardial performance. The heart responds by hypertrophic growth of cardiac myocytes, leading to increased cardiac muscle mass and enhanced cardiac performance. If the workload is not relieved and the heart can no longer meet the metabolic demands of the body, a pathological transition from hypertrophy to heart failure occurs, the hallmark feature of which is decreased cardiac contractility. It is thought that many of the same signaling pathways that regulate hypertrophy are involved in the progression to heart failure. Thus, understanding cellular signaling events that regulate cardiac growth and function may facilitate the elucidation of new therapeutic measures to prevent the development of heart failure.

Many laboratories, including our own, have used an in vitro cultured myocardial cell model to study the signaling molecules and pathways that are involved in the regulation of cardiac muscle cell hypertrophy. Hypertrophic growth of isolated neonatal rat ventricular myocytes is characterized by cell enlargement, upregulation of embryonic and contractile protein genes such as atrial natriuretic factor (ANF) and β-myosin heavy chain (β-MHC), and the assembly of myofibrils into organized sarcomeres (1). Studies emanating from the use of this cell model over the last decade have revealed central roles for the heterotrimeric G_q protein and the low-molecular-weight GTP-binding protein Ras in the regulation of agonist-induced hypertrophy (2–4). Transgenic mice have been generated that express wild-type $G\alpha_q$ (5) or activated Ras (6) in the heart. Both lines of mice developed cardiac hypertrophy (5, 6). Expression of constitutively activated $G\alpha_q$ or higher levels of wild-type $G\alpha_q$ resulted in the development of dilated cardiomyopathy and contractile failure, as did peripartal stress or pressure overload of $G\alpha_q$-expressing hearts (5, 7–9).

More recently, we and others have demonstrated that a Ras-related small G protein, RhoA, is also a key mediator of hypertrophic responses in ventricular myocytes (10–15). RhoA belongs to the Rho subfamily of GTP-binding proteins best known for their involvement in the regulation of the actin cytoskeleton. Specifically, RhoA has been shown to play a key role in both actin stress fiber formation and focal adhesion complex assembly in fibroblasts (reviewed in ref. 16). Our studies in neonatal rat ventricular myocytes suggested that RhoA function was required in α_1-adrenergic receptor–stimulated ANF and myosin light chain-2 (MLC-2) expression and myofibrillar organization. These responses were inhibited by a dominant-negative mutant of RhoA, as well as by the Rho-specific C3

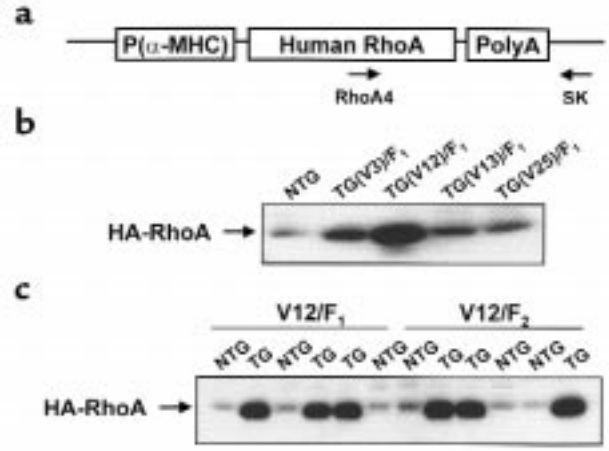

Figure 1
Identification of RhoA transgenic founder lines. (**a**) Schematic of transgenic vector showing inserted HA-tagged human RhoA cDNA and locations of primers used for genotyping by PCR. (**b**) Protein derived from whole hearts isolated from nontransgenic (NTG) and transgenic (TG) F_1 mice from the 4 founder lines (V3, V12, V13, and V25) was immunoblotted with anti-HA antibody, and bands were quantitated by densitometry. (**c**) Ventricular protein from 3 nontransgenic and 3 transgenic F_1 mice and 3 nontransgenic and 3 transgenic F_2 mice from the V12 founder line was immunoblotted with anti-HA antibody. A contaminating band at the approximate molecular weight of the HA-RhoA protein band was consistently observed in NTG lanes.

exoenzyme from *Clostridium botulinum* (10, 11). Conversely, a constitutively activated mutant of RhoA induced ANF expression and the organization of actin myofilaments into sarcomeric units (11). These data, together with those of other laboratories (12–15), suggested that RhoA was a mediator of hypertrophic responses in cardiomyocytes.

To investigate the role of RhoA in the intact heart, we generated transgenic mice overexpressing wild-type RhoA under the control of the cardiac-specific α-myosin heavy chain (α-MHC) promoter. Here we demonstrate that RhoA overexpression in the mouse heart induces sinus and atrioventricular (AV) nodal dysfunction and, ultimately, a lethal dilated cardiomyopathy associated with contractile failure.

Methods

Generation of RhoA transgenic mice. Hemagglutinin-tagged (HA-tagged) human wild-type and constitutively activated forms of RhoA cDNA (a gift from G. Bokoch, The Scripps Research Institute, La Jolla, California, USA) were subcloned into a pBluescript-based transgenic vector between the 5.5-kb murine α-MHC promoter (a gift from. J. Robbins, University of Cincinnati, Cincinnati, Ohio, USA) and 250-bp SV-40 polyadenylation sequences. Purified transgene fragments were injected into the male pronuclei of fertilized mouse oocytes. The resulting pups were screened for the presence of the transgene by PCR, using a RhoA-specific primer RhoA4 (5′-GCCCATCATCCTAGTTGGGAA-3′) and a transgenic vector-specific primer SK (5′-CGCTCTAGAACTAGTGGATC-3′), as indicated in Figure 1a. Briefly, tail samples were digested in lysis buffer (75 mM NaCl, 25 mM EDTA, 10 mM Tris [pH 8.0], 1% SDS) and 0.4 mg/mL proteinase K. Genomic DNA was precipitated with isopropanol. PCR was performed as follows: 95°C for 30 seconds, 60°C for 30 seconds, and 72°C for 1 minute for 35 cycles, with a final extension step at 72°C for 10 minutes.

Western blotting. Freshly removed hearts were weighed and immediately frozen in liquid nitrogen. Proteins were extracted from tissue as described previously (17). Briefly, frozen tissue was powdered and homogenized in ice-cold lysis buffer. Protein concentration was determined by Bradford analysis, and 60 μg of protein was boiled with Laemmli buffer and electrophoresed on a 15% SDS polyacrylamide gel. Gels were electroblotted onto Immobilon-P membranes (Millipore Corp., Bedford, Massachusetts, USA). Membranes were blocked in 3% BSA/0.1% Tween/PBS, incubated with mouse anti-RhoA (Santa Cruz Biotechnology Inc., Santa Cruz, California, USA) or mouse anti-HA (Roche Molecular Biochemicals, Indianapolis, Indiana, USA) antibody, followed by secondary horseradish peroxidase–conjugated goat anti-mouse IgG antibody (Sigma Chemical Co., St. Louis, Missouri, USA). Enhanced chemiluminescence was performed using the SuperSignal Chemiluminescent Detection System (Pierce Chemical Co., Rockford, Illinois, USA).

Histology. Tissues were fixed in 3.7% formaldehyde/PBS overnight and then dehydrated in 70% ethanol, embedded in paraffin wax, and sectioned. Tissue sections were stained with hematoxylin/eosin or Masson's trichrome. For cell size measurements, transverse sections were stained with TRITC-labeled wheat germ agglutinin (Sigma Chemical Co.), and a cross-sectional area (short axis) of myocytes in the left ventricular free wall was determined using the Image Proplus software program as described previously (5).

RNA dot blot analysis. RNA was prepared from ventricular tissue using Trizol reagent (GIBCO BRL, Gaithersburg, Maryland, USA) according to the manufacturer's protocol and as described previously (5, 18). The RNA (2–3 μg per dot) was blotted onto Hybond Nylon+ membranes (Amersham Phar-

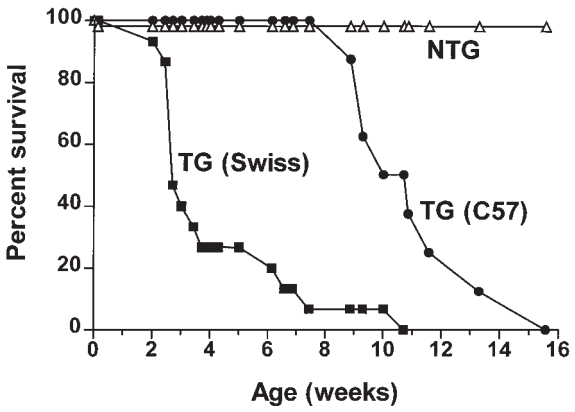

Figure 2
Survival analysis of RhoA transgenic mice. F_1 heterozygotes were generated by backcrossing the V12 founder mouse with either Black Swiss or C57BL/6 mice. The open triangles represent percent survival of nontransgenic (NTG) F_1 mice (n = 55); the filled squares represent survival of transgenic (TG) V12 × Black Swiss F_1 mice (n = 15); the filled circles represent survival of transgenic V12 × C57BL/6 F_1 mice (n = 8).

macia Biotech Inc., Piscataway, New Jersey, USA) using the Bio-Dot apparatus (Bio-Rad Laboratories Inc., Hercules, California, USA) and was probed with gene transcript–specific antisense oligonucleotide probes to GAPDH, α-MHC, β-MHC, α-skeletal actin, ANF, sarcoplasmic reticulum Ca^{2+}-ATPase (SERCA), phospholamban, and α-cardiac actin as described (18). Radiolabeled RNA dots were quantitated on a PhosphorImager or by AMBIS radioanalytic scanning. Data were normalized to GAPDH.

Transthoracic echocardiography. Mice were anesthetized by intraperitoneal injection of avertin (2.5%, 14 μL/g). Echocardiograms were obtained using an Apogee CX unit (ATL Interspec, Bothell, Washington, USA) as described previously (19).

Electrocardiographic assessment. Mice were anesthetized by intraperitoneal injection of ketamine (0.033 g/kg) and pentobarbital (0.015 g/kg). Needle electrodes (27 gauge) were placed subcutaneously in each limb to obtain a 6 limb-lead electrocardiogram using a Mac I electrocardiograph (ECG) machine (Marquette Electronics Inc., Milwaukee, Wisconsin, USA). For atropine and isoproterenol studies, basal ECG recordings were obtained before and 10 minutes after intraperitoneal administration of drugs (0.5 mg/kg atropine or 2.0 mg/kg isoproterenol).

Results

Cardiac overexpression of RhoA results in premature mortality. Transgenic mice expressing wild-type RhoA under the control of the cardiomyocyte-specific α-MHC promoter were generated as described in Methods. Four wild-type RhoA transgenic founders were identified by PCR. These transgene-carrying founders were bred with Black Swiss or C57BL/6 mice to generate F_1 heterozygotes. Myocardial transgenic RhoA protein-expression levels were determined in F_1 heterozygotes (Figure 1b). Whereas V13 and V25 progeny displayed only a marginal increase in total RhoA content (~1.5-fold increase over nontransgenic RhoA levels), the V3 founder line showed an ~4-fold increase and the V12 founder line showed an ~20-fold increase. The levels of expression of the transgenic RhoA protein were further observed to be similar among transgenic littermates from the V12 founder line and between transgenic F_1- and F_2-generation mice (Figure 1c), indicating a single site of transgene integration.

Transgenic F_1 heterozygotes, generated by backcrossing the highest-expressing wild-type RhoA founder mouse (V12) with Black Swiss mice, were prone to premature death, the majority dying between 3 and 7 weeks after birth (Figure 2). When F_1 heterozygotes were generated by backcrossing the transgenic founder with C57BL/6 rather than Black Swiss mice, mortality was delayed. The transgenic progeny still died over a 4-week period, but survival was prolonged in the C57BL/6 background mice, with 50% of transgenic pups surviving to 11 weeks, as compared with 3 weeks of age for pups in the Black Swiss background (Figure 2).

Transgenic mice expressing a constitutively activated form of RhoA in the myocardium were also generated. One transgene-carrying founder mouse died at 12 weeks of age and could not be bred. Another founder mouse, VB25, produced F_1 heterozygotes that showed significant expression of activated RhoA protein, albeit at levels less than that of wild-type RhoA in the V12 founder line (Figure 3). These activated RhoA-express-

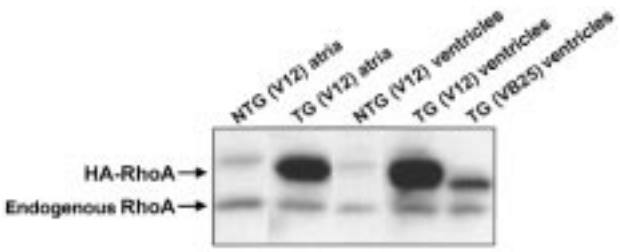

Figure 3
Transgenic RhoA is exressed in atria as well as ventricles. Lysates from atria and ventricles of nontransgenic (NTG) and transgenic (TG) F_1 heterozygotes from the V12 wild-type RhoA founder line and the VB25 activated RhoA founder line were immunoblotted with anti-RhoA antibody. A faint contaminating band at the approximate molecular weight of the HA-RhoA protein band was consistently observed in NTG lanes.

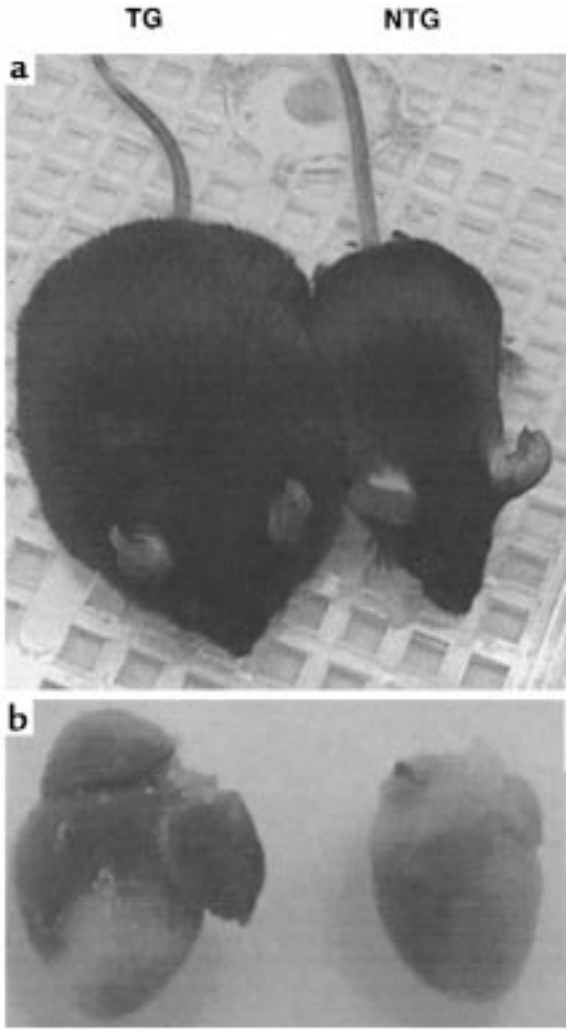

Figure 4
Generalized edema and atrial enlargement in RhoA transgenic mice. Images of nontransgenic (NTG) and RhoA transgenic (TG) littermates (**a**) and their hearts (**b**) were captured using a Sony Mavica digital camera. Note the bloated appearance of the transgenic mouse (**a**) and the massively enlarged atria in the transgenic heart (**b**).

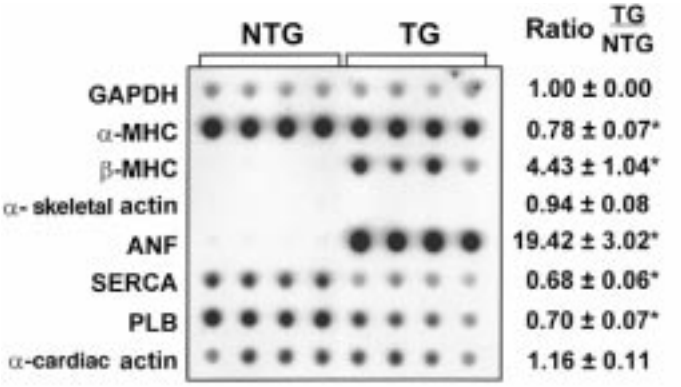

Figure 5
Ventricular gene expression in RhoA transgenic mice. RNA isolated from ventricular tissue of nontransgenic (NTG) and transgenic (TG) mice was subjected to dot blot analysis using gene transcript–specific antisense oligonucleotide probes as indicated. A representative autoradiograph is shown, with each vertical column of 8 dots representing ventricular RNA from 1 animal. GAPDH was used as the normalizing control in each experiment and was unchanged between nontransgenic and transgenic samples. Consistent with our genotyping results, only RNA from RhoA transgenic mice showed intense hybridization with a RhoA probe (data not shown). The levels of each transcript in transgenic samples (right) were calculated as a ratio of the levels seen in nontransgenic mice, with a mean value of >1 representing induction and a value of <1 representing inhibition of gene expression in transgenic mice relative to nontransgenic mice. Data are presented as the mean ± SE (NTG: $n = 7$; TG: $n = 7$). *$P < 0.05$ TG vs. NTG.

ing mice also manifested the phenotype of sudden and premature death and were included in some of the experiments described below.

The lethality of the phenotype warranted confirmation that there was no detectable expression of RhoA in noncardiac tissue. Western blots of extracts from brain, kidney, liver, lung, and spleen with anti-RhoA and anti-HA antibodies revealed no expression of the transgene in any of these tissues (data not shown), consistent with prior observations that the α-MHC promoter specifies cardiac-restricted transgene expression (20). Comparable levels of RhoA transgene expression were detected in atrial and ventricular tissue of transgene-positive mouse hearts from the V12 founder line (Figure 3).

Cardiac overexpression of RhoA results in increased atrial weight and ventricular expression of ANF and β-MHC genes. The onset of death in the RhoA transgenic mice was often very sudden. Just prior to death, the mice appeared dyspneic and weak. In most cases, varying degrees of generalized edema were observed. In severe cases, the mice took on the characteristic bloated appearance of anasarca (Figure 4a). To obtain evidence of hypertrophy in the wild-type RhoA transgenic mice, they were sacrificed within 1 week of onset of signs of progressive disease. Hearts from RhoA transgenic mice showed a moderate but significant increase in heart weight normalized to tibial length (Table 1). Heart weight was normalized to tibial length rather than body weight because of the presence of variable and widespread edema that increased body weight in some animals. Surprisingly, when the cardiac chambers were dissected and weighed separately, the increase in heart weight was determined to be due to a specific increase in atrial, rather than ventricular, weight (Table 1). Consistent with the observed increase in atrial weight, RhoA transgenic hearts showed significant atrial enlargement compared with hearts from nontransgenic littermates (Figure 4b).

Specific alterations in cardiac gene expression have been associated with hypertrophic heart disease. To determine if RhoA overexpression altered the genetic program of the heart, we isolated RNA from mouse ventricles and examined the expression of a selected panel of genes by dot blot analysis. As shown in Figure 5, transgenic ventricles showed significantly increased ANF and β-MHC mRNA levels compared with control nontransgenic ventricles, but mRNA levels of another hypertrophic marker, α-skeletal actin, were unchanged. There was a modest but significant decrease in α-MHC, SERCA, and phospholamban (PLB) mRNA levels (Figure 5). A similar pattern of gene expression was seen in control samples processed from ventricles from $G\alpha_q$ transgenic mice (5), except that α-skeletal actin mRNA levels were also increased in ventricular tissue from $G\alpha_q$ transgenic mice.

Cardiac overexpression of RhoA results in ventricular dilation and dysfunction. Histological analysis of hearts obtained from mice sacrificed within 1 week of onset of overt disease demonstrated dilation of both cardiac ventricular chambers (Figure 6, a and b). Wheat germ agglutinin labeling of cell membranes from sections of the left ventricular free wall illustrated heterogeneity in transgenic (TG) cardiomyocyte dimensions, without a statistically significant increase in overall cell size, as compared with nontransgenic (NTG) samples (Figure 6, c and d; NTG: 199 ± 38 μm^2, TG: 215 ± 96 μm^2). Masson's trichrome staining revealed the presence of interstitial fibrosis (blue staining), but no inflammation, in the transgenic heart (Figure 6, e and f). In addition, there was an abnormal accumulation of red blood cells in the liver, indicative of acute hepatic congestion (Figure 6, g and h). These findings, together with the observed alterations in ventricular gene expression, are consistent with the pathology generally associated with dilated cardiomyopathy.

To determine if ventricular dysfunction accompanied ventricular dilation, the effects of RhoA overexpression on cardiac function were assessed by echocardiography.

Table 1
Morphometric analysis of transgenic mice

Ratio	Nontransgenic	Transgenic
Heart weight/tibial length	0.66 ± 0.03 ($n = 33$)	0.82 ± 0.04[A] ($n = 30$)
Atrial weight/tibial length	0.60 ± 0.10 ($n = 9$)	1.81 ± 0.17[A] ($n = 8$)
Ventricular weight/tibial length	0.72 ± 0.07 ($n = 9$)	0.70 ± 0.07 ($n = 8$)

Whole hearts were excised from nontransgenic mice (NTG) and sick transgenic mice (TG), weighed and normalized to tibial length (heart weight/tibial length ratio). For a subset of these animals, following measurement of whole-heart weight, atria were dissected and weighed separately, and the ratio to tibial length was calculated. Ventricular weight was calculated by subtracting atrial weight from heart weight. Data are presented as the mean ± SE. [A]$P < 0.005$ TG vs. NTG.

Echocardiographic analysis of the mice prior to development of overt ventricular failure (TG-healthy) revealed an insignificant trend toward diminished left ventricular contractile function, as assessed by fractional shortening (Table 2). However, when mice developed proptosis, edema, and lethargy (TG-sick), markedly depressed left ventricular fractional shortening was demonstrable by echocardiography (25.2% FS in TG-sick vs. 37.5% in NTG; Table 2). A trend toward thinning of the left ventricular septal (SEPth) and posterior (PWth) walls was also observed in RhoA transgenic mice (Table 2). Thus, the echocardiographic data are also consistent with the manifestation of dilated cardiomyopathy in RhoA transgenic mice.

Cardiac overexpression of RhoA results in pacemaker/AV conduction defects. In the course of the echocardiographic analysis, it was noted that the heart rates of all transgenic mice analyzed were markedly depressed (Table 2). This was evident in healthy as well as overtly sick mice. These findings were confirmed by ECG analysis. As shown in Table 3, the heart rate in the high-level RhoA transgenic mice (TG-high) was significantly lower than that in nontransgenic mice. The ECG tracings from 2 of these transgenic mice exhibited greatly prolonged PR intervals, indicative of second-degree AV block (Figure 7c and Table 3). Three other mice from the same founder line showed no distinct P waves and narrow QRS complexes, indicative of atrial fibrillation with impaired AV conduction (Figure 7b and Table 3). Statistically significant bradycardia was also observed in mice expressing wild-type RhoA at lower levels (TG-low; Table 3), with more than 30% showing a heart rate slower than 450 bpm, compared with 6% of nontransgenic mice. Mice expressing a constitutively activated form of RhoA (TG-act) also demonstrated depressed heart rates (Table 3). ECG recordings from 3 of the 4 activated RhoA mice analyzed demonstrated P waves of varying shape, a characteristic of wandering pacemaker activity (Table 3).

To explore further the basis for the apparent defect in sinus nodal function, we examined the responses to muscarinic cholinergic receptor blockade. Intraperitoneal administration of atropine (0.5 mg/kg) caused the expected marked positive chronotropic response in control nontransgenic mice (Figure 7e). Notably, the bradycardia in RhoA transgenic mice was not reversed. Indeed, a paradoxical enhancement of the bradycardia was seen. The ECG tracings were further analyzed to rule out the possibility that atropine increased the sinoatrial (SA) nodal rhythm but failed to affect ventricular rate because of AV block. In ECG tracings where clear P waves were evident, no increase in atrial rate (P-wave frequency) was observed following atropine administration (Figure 7d). This observation is shown graphically in Figure 7f. Despite the lack of positive chronotropic response to atropine, RhoA transgenic mice did show an increase in heart rate (from 331 bpm to 471 bpm; data not shown) in response to β-adrenergic receptor stimulation with isoproterenol. This observation confirmed that the hearts were functionally competent to beat at higher rates. Taken together, the ECG and echocardiographic data demonstrate that RhoA transgenic mice have severe bradycardia, apparently resulting from alterations in SA and AV nodal function, and rapidly develop ventricular dysfunction and failure.

Discussion

To demonstrate a signaling role for RhoA in control of myocardial growth and function in vivo, we generated transgenic mice specifically overexpressing RhoA in the myocardium. We employed the α-MHC pro-

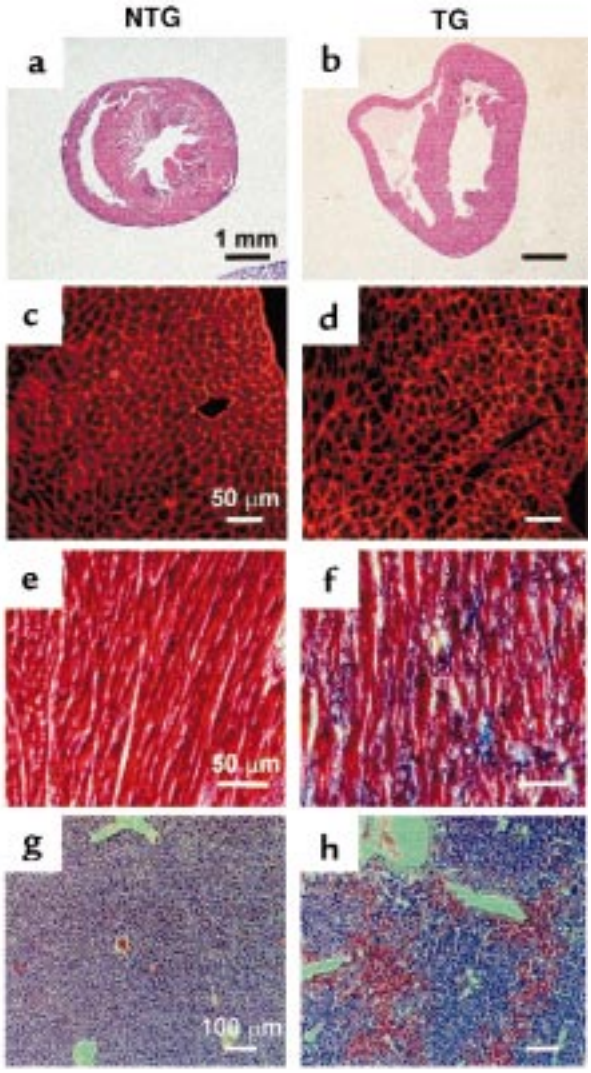

Figure 6
Cardiac and hepatic pathology in RhoA transgenic mice. Hematoxylin and eosin–stained transverse sections of nontransgenic (**a**) and transgenic (**b**) hearts demonstrate dilation of right and left ventricular chambers in transgenic hearts. TRITC-conjugated, wheat germ agglutinin–labeled cell membranes show uniform cell size in nontransgenic samples (**c**) and heterogeneous cell size and interstitial fibrosis in transgenic samples (**d**). High-power magnification of Masson's trichrome–stained sections taken from the left ventricular free wall demonstrates normal staining in nontransgenic samples (**e**) and massive fibrosis, as indicated by the blue staining, in transgenic samples (**f**). Liver sections stained with hematoxylin and eosin show normal staining in nontransgenic samples (**g**) but blood congestion in transgenic samples (**h**). Scale bars are as indicated.

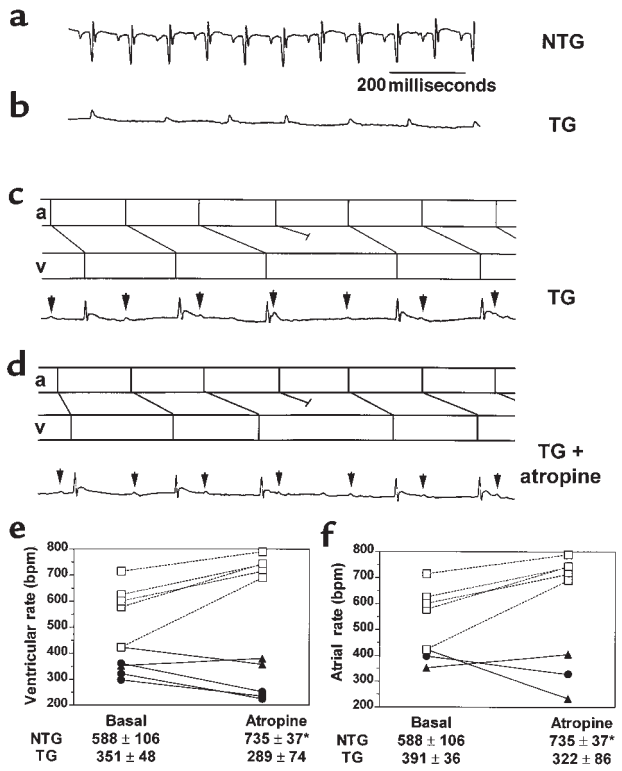

Figure 7

RhoA transgenic mice have slow heart rate and fail to respond to atropine. Representative ECG recordings from an anesthetized nontransgenic (NTG) mouse (**a**) and an anesthetized RhoA transgenic (TG) mouse with atrial fibrillation (**b**) or AV block before (**c**) and after (**d**) intraperitoneal atropine administration. All ECG tracings are to the same scale as indicated in **a**. In **c** and **d**, P waves are indicated by arrows; atrial (a) and ventricular (v) depolarizations are depicted in the ladder diagrams, as shown above each recording. Ventricular rates (**e**) and, where possible, atrial rates (**f**), were determined for nontransgenic (open squares), wild-type RhoA transgenic (filled circles), and constitutively activated RhoA transgenic (filled triangles) mice at basal conditions and following intraperitoneal atropine administration. Ventricular rates (NTG: $n = 5$; TG: $n = 5$) or atrial rates (NTG: $n = 5$; TG: $n = 3$), presented as mean ± SD for each condition, are indicated below the respective graphs. *$P < 0.02$ atropine vs. basal.

moter, which has been widely used to obtain cardiac-specific transgene expression in mice, and confirmed that transgene expression was restricted to the heart. Of the 4 wild-type RhoA-overexpressing founder lines identified, premature mortality was observed only in the line showing the highest level of RhoA overexpression, with genetic background playing a significant role in determining the onset of lethality. Similar pathology was detected in mice expressing the GTPase-deficient, constitutively activated form of RhoA in the heart. A founder mouse and 2 other transgenic mice from a different founder line expressing activated RhoA died prematurely and showed atrial enlargement, increased heart weight, and dilation of ventricular chambers. Whereas overt heart failure developed only in the highest-expressing wild-type or activated RhoA transgenic mice, bradycardia was also demonstrated in mice expressing lower levels of wild-type or activated RhoA. Notably, bradycardia was evident prior to the onset of overt ventricular disease. Thus, phenotypic manifestations of RhoA overexpression were observed in at least 5 different lines and appear to be dependent on a threshold, with bradycardia occurring at a lower threshold than development of ventricular failure.

These findings suggest that the primary effect of RhoA overexpression is sinus or AV dysfunction, which eventually culminates in ventricular failure. Although echocardiographic data could be obtained from only 2 animals both prior to and subsequent to the onset of overt signs of disease, both mice showed bradycardia even at the presymptomatic stage, whereas a marked decline in left ventricular contractile function was evident only at the symptomatic stage. Because the markedly reduced heart rate in RhoA transgenic mice could result in a compensatory increase in fractional shortening to maintain constant cardiac output, the actual depression of contractile function in the RhoA transgenic mice may be even more severe than is apparent.

Ventricular reinduction of ANF, β-MHC, and α-skeletal actin gene expression are characteristics associated with a variety of murine models of cardiac hypertrophy. However, the lack of effect of RhoA on myocardial cell size, and the absence of significant increases in ventricular mass, indicates that RhoA overexpression does not cause ventricular hypertrophy. It is also of interest in this regard that whereas ventricular ANF and β-MHC gene expression are increased in the RhoA-overexpressing mouse, α-skeletal actin gene expression is not upregulated. A recent study using a transgenic mouse model of hypertrophic cardiomyopathy demonstrated that ventricular ANF induction was localized in areas of tissue pathology and fibrosis and dissociated from hypertrophy (21). Because hearts from RhoA-overexpressing mice show obvious tissue pathology based on the presence of ventricular fibrosis, this might explain the upregulation of ventricular ANF gene expression. Why expression of the β-MHC gene is upregulated, whereas that of the α-skeletal actin gene is not, remains to be elucidated. The downregulation of the α-MHC, SERCA, and phospholamban genes seen in RhoA-overexpressing mice is characteristic not only of hypertrophied myocardium but also of end-stage failing myocardium (22–26).

While the α-MHC promoter is generally used to drive postnatal transgene expression in the ventricle, expression of the α-MHC promoter in the atria occurs during embryonic development as well as postnatally (27, 28). We observed marked increases in RhoA expression in atrial and ventricular tissue from RhoA transgenic mice. The early atrial RhoA expression is probably responsible for the predominantly atrial phenotype observed. This could explain the discordance between our in vitro data, which suggested that RhoA regulates ventricular cardiomyocyte hypertrophy, and our in vivo data, which demonstrated that RhoA overexpression or hyperactivation causes ventricular dilation and failure. These latter manifesta-

tions may occur secondary to development of the atrial phenotype and thus may not reflect a primary role of RhoA in ventricular function and regulation.

Atrial enlargement and striking defects in sinus and AV conduction were evident in the ECG recordings from RhoA transgenic mice. While increases in atrial size have been seen in several other murine transgenic models and may, in part, be secondary to left ventricular dysfunction (6), accompanying alterations in heart rate or rhythm have been described in only a few of these mice. Of note, cardiac-specific overexpression of the angiotensin AT_1 receptor led to an ~9-fold increase in atrial weight, bradycardia, and abnormal AV conduction (27). The early lethality of these animals was attributed to atrial enlargement because no significant ventricular phenotype was observed. On the other hand, calmodulin overexpression led to an ~3-fold increase in atrial weight, but heart rate was unchanged and no atrial or ventricular arrhythmias were detected (29). These studies dissociate atrial size increases from heart rate or rhythm abnormalities, and indicate that atrial enlargement does not necessarily result in bradycardia. Moreover, while bradycardia has been observed in $G\alpha_q$ transgenic mice (5), no defects in pacemaker or AV conduction are evident in these animals. Hypertrophy in the Ras or *MLP*$^{-/-}$ mouse models is also lacking atrial rhythm defects.

We hypothesize that overexpression of RhoA in the myocardium results in SA and AV nodal dysfunction due to a specific effect of RhoA on the ion channels regulating cardiac cell excitation and conduction. This hypothesis emanates from a recent study demonstrating the regulation of a delayed rectifier potassium channel, Kv1.2, by RhoA (30). This channel, which was cloned from adult rat heart atrium (31), is regulated through G_q-coupled muscarinic cholinergic receptors, at least in part through tyrosine phosphorylation (32). Interestingly, RhoA was found to physically associate with and suppress the activity of Kv1.2 (30). Delayed rectifier potassium channels participate in the repolarization of action potentials. Suppression due to RhoA overexpression or hyperactivation would, therefore, be predicted to prolong cardiac action potentials and thereby result in decreased SA nodal rate. Preliminary experiments in which RhoA is immunoprecipitated from lysates demonstrate a physical association between Kv1.2 and RhoA in neonatal rat ventricular myocytes and in mouse atria and ventricles (data not shown).

Another potential mechanism by which RhoA could induce bradycardia would be through activation of the inward rectifying potassium channels in atrial pacemaker cells (reviewed in ref. 33). Parasympathetic stimulation of atrial M_2 muscarinic cholinergic receptors activates these channels and slows heart rate through hyperpolarization of pacemaker cells in the SA and AV nodes. Our finding that atropine fails to reverse the bradycardia induced by RhoA overexpression suggests that this normal channel might be dysregulated, i.e., that it is constitutively activated and therefore remains "on" even in the absence of its normal parasympathetic muscarinic regulation.

Table 2
Echocardiographic analysis of transgenic mice

	LVEDD (mm)	LVESD (mm)	FS (%)	SEPth (mm)	PWth (mm)	mVCFc (circ/s)	HR (bpm)
NTG (n = 6)							
Mean	3.35	2.09	37.5	0.68	0.71	2.45	402.2
SD	0.38	0.21	3.6	0.11	0.10	0.36	86.2
TG-healthy (n = 5)							
Mean	3.10	2.05	33.8	0.62	0.64	2.44	195.9[A]
SD	0.19	0.15	1.4	0.09	0.08	0.34	102.1
TG-sick (n = 3)							
Mean	3.60	2.71	25.2[A]	0.56	0.59	1.68[A]	233.4
SD	0.36	0.48	5.6	0.05	0.12	0.28	126.3

Echocardiographic analysis of 9- to 11-week-old nontransgenic (NTG) and transgenic (TG) healthy (presymptomatic) and sick (showing signs of edema or lethargy) F_1-generation mice from the V12 founder line. LVEDD, left ventricular end-diastolic diameter; LVESD, left ventricular end-systolic diameter; FS, percent fractional shortening calculated as 100 × [(LVEDD – LVESD)/LVEDD]; SEPth, ventricular septal thickness; PWth, posterior wall thickness; mVCFc, heart rate–corrected mean velocity of circumferential shortening; HR, heart rate. [A]$P < 0.05$ TG (healthy or sick) vs. NTG.

To elucidate the mechanism by which RhoA functions to regulate pacemaker activity and ventricular contractile function, we have begun to generate a new line of transgenic mice that will express the RhoA transgene in a conditional manner. This strategy, based on the *cre*-lox technology, should ensure preservation of viability in the founder generation. Expression of the transgene will be accomplished by breeding the founder mice with mice that express the *cre* recombinase protein in either the ventricular chambers or in the atria and ventricles, as specified by the endogenous promoters (34). This expression will further allow us to differentiate the effects of RhoA overexpression in atrial and ventricular tissue and will provide insight into the relative roles of RhoA in affecting atrial and ventricular function.

Table 3
Electrocardiographic analysis of transgenic mice

	NTG (n = 16)	TG-high (n = 5)	TG-act (n = 4)	TG-low (n = 19)
Heart rate (bpm)	567 ± 19	323 ± 26[A]	424 ± 34[A]	493 ± 25[A]
PQ interval (ms)	32.3 ± 0.6	49.0 ± 1.0[A]	35.0 ± 1.1	33.0 ± 0.9
QRS interval (ms)	20.7 ± 0.5	23.0 ± 1.2	21.0 ± 2.8	21.8 ± 2.8
QT interval (ms)	55.5 ± 1.6	78.8 ± 14.5[A]	66.0 ± 2.3	60.5 ± 2.2
QTc interval	53.5 ± 1.0	55.9 ± 6.4	55.2 ± 2.1	53.9 ± 1.3
Number of mice with:				
second-degree AV block	0	2	2	0
atrial fibrillation	0	3	0	0
wandering pacemaker	0	0	3	1
heart rate <450 bpm	0	5	3	6

Electrocardiographic analysis of nontransgenic mice (NTG), wild-type RhoA transgenic mice from the high-level overexpressing V12 founder line (TG-high; F_2 generation), the low-level overexpressing V3 founder line (TG-low; F_1 generation), and activated RhoA transgenic F_1 mice (TG-act; F_1 generation). Because P waves were indiscernible in 3 of the TG-high mice, the PQ interval data represent data from the 2 mice in which clear P waves were observed. QTc interval is the heart rate–corrected QT interval. Data are presented as the mean ± SE. [A]$P < 0.05$ TG vs. NTG.

Acknowledgments

The authors would like to thank A. Canning, J. Contos, N. Dalton, M. Davis, D. Goldstein, M. Tsang, J. Weiner, J. Adams, V. Bhargava, J. Chun, M. Hoshijima, A. Morielli, E. Peralta, and Y. Wang for reagents, equipment, technical assistance, and useful discussions. Valerie P. Sah is supported by an American Heart Association-Western States Affiliate Predoctoral Fellowship. This work was supported in part by National Institutes of Health grants HL-28143 (to J.H. Brown) and HL-46345 (to J.H. Brown, K.R. Chien, and J. Ross Jr.).

1. Chien, K.R., Knowlton, K.U., Zhu, H., and Chien, S. 1991. Regulation of cardiac gene expression during myocardial growth and hypertrophy: molecular studies of an adaptive physiologic response. *FASEB J.* **5**:3037–3046.
2. Thorburn, A., et al. 1993. H-Ras-dependent pathways can activate morphological and genetic markers of cardiac muscle cell hypertrophy. *J. Biol. Chem.* **268**:2244–2249.
3. Thorburn, A. 1994. Ras activity is required for phenylephrine-induced activation of mitogen-activated protein kinase in cardiac muscle cells. *Biochem. Biophys. Res. Commun.* **205**:1417–1422.
4. LaMorte, V.J., et al. 1994. G_q- and Ras-dependent pathways mediate hypertrophy of neonatal rat ventricular myocytes following α_1-adrenergic stimulation. *J. Biol. Chem.* **269**:13490–13496.
5. D'Angelo, D.D., et al. 1997. Transgenic $G\alpha_q$ overexpression induces cardiac contractile failure in mice. *Proc. Natl. Acad. Sci. USA.* **94**:8121–8126.
6. Hunter, J.J., Tanaka, N., Rockman, H.A., Ross, J., Jr., and Chien, K.R. 1995. Ventricular expression of a MLC-2/v-Ras fusion gene induces cardiac hypertrophy and selective diastolic dysfunction in transgenic mice. *J. Biol. Chem.* **270**:23173–23178.
7. Mende, U., et al. 1998. Transient cardiac expression of constitutively active $G\alpha_q$ leads to hypertrophy and dilated cardiomyopathy by calcineurin-dependent and independent pathways. *Proc. Natl. Acad. Sci. USA.* **95**:13893–13898.
8. Sakata, Y., Hoit, B.D., Liggett, S.B., Walsh, R.A., and Dorn, G.W. 1998. Decompensation of pressure overload hypertrophy in $G\alpha_q$ overexpressing mice. *Circulation.* **97**:1488–1495.
9. Adams, J.W., et al. 1998. Enhanced $G\alpha_q$ signaling: a common pathway mediates cardiac hypertrophy and apoptotic heart failure. *Proc. Natl. Acad. Sci. USA.* **95**:10140–10145.
10. Sah, V.P., Hoshijima, M., Chien, K.R., and Brown, J.H. 1996. Rho is required for $G\alpha_q$ and α_1-adrenergic receptor signaling in cardiomyocytes: dissociation of Ras and Rho pathways. *J. Biol. Chem.* **271**:31185–31195.
11. Hoshijima, M., Sah, V.P., Wang, Y., Chien, K.R., and Brown, J.H. 1998. The low molecular weight GTPase Rho regulates myofibril formation and organization in neonatal rat ventricular myocytes: involvement of Rho kinase. *J. Biol. Chem.* **273**:7725–7730.
12. Thorburn, J., Xu, S., and Thorburn, A. 1997. MAP kinase- and Rho-dependent signals interact to regulate gene expression but not actin morphology in cardiac muscle cells. *EMBO J.* **16**:1888–1900.
13. Wang, S.-M., Tsai, Y.-J., Jiang, M.-J., and Tseng, Y.-Z. 1997. Studies on the function of RhoA protein in cardiac myofibrillogenesis. *J. Cell. Biochem.* **66**:43–53.
14. Aoki, H., Izumo, S., and Sadoshima, J. 1998. Angiotensin II activates RhoA in cardiac myocytes: a critical role of RhoA in angiotensin II-induced premyofibril formation. *Circ. Res.* **82**:666–676.
15. Hines, W.A., and Thorburn, A. 1998. Ras and Rho are required for $G\alpha_q$-induced hypertrophic gene expression in neonatal rat cardiac myocytes. *J. Mol. Cell. Cardiol.* **30**:485–494.
16. Mackay, D.J.G., and Hall, A. 1998. Rho GTPases. *J. Biol. Chem.* **273**:20685–20688.
17. Ramirez, M.T., et al. 1997. The MEKK-JNK pathway is stimulated by α_1-adrenergic receptor and Ras activation and is associated with in vitro and in vivo cardiac hypertrophy. *J. Biol. Chem.* **272**:14057–14061.
18. Jones, W.K., et al. 1996. Ablation of the murine α myosin heavy chain gene leads to dosage effects and functional deficits in the heart. *J. Clin. Invest.* **98**:1906–1917.
19. Tanaka, N., et al. 1996. Transthoracic echocardiography in models of cardiac disease in the mouse. *Circulation.* **94**:1109–1117.
20. Subramaniam, A., et al. 1991. Tissue-specific regulation of the alpha-myosin heavy chain gene promoter in transgenic mice. *J. Biol. Chem.* **266**:24613–24620.
21. Vikstrom, K.L., Bohlmeyer, T., Factor, S.M., and Leinwand, L.A. 1998. Hypertrophy, pathology, and molecular markers of cardiac pathogenesis. *Circ. Res.* **82**:773–778.
22. Nakao, K., Minobe, W., Roden, R., Bristow, M.R., and Leinwand, L.A. 1997. Myosin heavy chain gene expression in human heart failure. *J. Clin. Invest.* **100**:2362–2370.
23. Mercadier, J.J., et al. 1990. Altered sarcoplasmic reticulum Ca^{2+}-ATPase gene expression in the human ventricle during end-stage heart failure. *J. Clin. Invest.* **85**:305–309.
24. Hasenfuss, G., et al. 1994. Relation between myocardial function and expression of sarcoplasmic reticulum Ca^{2+}-ATPase in failing and nonfailing human myocardium. *Circ. Res.* **75**:434–442.
25. Meyer, M., et al. 1995. Alterations of sarcoplasmic reticulum proteins in failing human dilated cardiomyopathy. *Circulation.* **92**:778–784.
26. Schaub, M.C., Hefti, M.A., Harder, B.A., and Eppenberger, H.M. 1997. Various hypertrophic stimuli induce distinct phenotypes in cardiomyocytes. *J. Mol. Med.* **75**:901–920.
27. Hein, L., et al. 1997. Overexpression of angiotensin AT_1 receptor transgene in the mouse myocardium produces a lethal phenotype associated with myocyte hyperplasia and heart block. *Proc. Natl. Acad. Sci. USA.* **94**:6391–6396.
28. Colbert, M.C., et al. 1997. Cardiac compartment-specific overexpression of a modified retinoic acid receptor produces dilated cardiomyopathy and congestive heart failure in transgenic mice. *J. Clin. Invest.* **100**:1958–1968.
29. Gruver, C.L., DeMayo, F., Goldstein, M.A., and Means, A.R. 1993. Targeted developmental overexpression of calmodulin induces proliferative and hypertrophic growth of cardiomyocytes in transgenic mice. *Endocrinology.* **133**:376–388.
30. Cachero, T.G., Morielli, A.D., and Peralta, E. 1998. The small GTP-binding protein RhoA regulates a delayed rectifier potassium channel. *Cell.* **93**:1077–1085.
31. Paulmichl, M., et al. 1991. Cloning and expression of a rat cardiac delayed rectifier potassium channel. *Proc. Natl. Acad. Sci. USA.* **88**:7892–7895.
32. Huang, X.-Y., Morielli, A.D., and Peralta, E. 1993. Tyrosine kinase-dependent suppression of a potassium channel by the G protein-coupled m1 muscarinic acetylcholine receptor. *Cell.* **75**:1145–1156.
33. Brown, A.M., and Birnbaumer, L. 1990. Ionic channels and their regulation by G protein subunits. *Annu. Rev. Physiol.* **52**:197–213.
34. Chen, J., et al. 1998. Selective requirement of myosin light chain-2v in embryonic heart function. *J. Biol. Chem.* **273**:1252–1256.